NACA RM E57A31

NACA

RESEARCH MEMORANDUM

FULL-SCALE FREE-JET INVESTIGATION OF A TWO-SHOCK SIDE-INLET DIFFUSER AT MACH 2.75 AND A COMPARISON WITH A SINGLE-SHOCK DIFFUSER

By John E. McAulay

Lewis Flight Propulsion Laboratory
Cleveland, Ohio

NATIONAL ADVISORY COMMITTEE
FOR AERONAUTICS

WASHINGTON
April 24, 1957
Declassified October 28, 1960

NACA RM E57A31

NATIONAL ADVISORY COMMITTEE FOR AERONAUTICS

RESEARCH MEMORANDUM

FULL-SCALE FREE-JET INVESTIGATION OF A TWO-SHOCK SIDE-INLET DIFFUSER AT MACH 2.75 AND A COMPARISON WITH A SINGLE-SHOCK DIFFUSER

By John E. McAulay

SUMMARY

A full-scale free-jet investigation of a two-shock side-inlet diffuser at a Mach number of 2.75 was conducted in an NACA Lewis laboratory altitude test chamber. Data were obtained over ranges of free-stream total pressure and temperature of 3800 to 1930 pounds per square foot and 860° to 990° R, respectively. All data were obtained at a nominal inlet Mach number of 2.75 and an angle of attack of zero.

The supercritical mass-flow ratio of the two-shock inlet diffuser was about 0.99, and its critical pressure recovery was 0.643. A single-shock diffuser also designed for a Mach number of 2.75 had values of mass-flow ratio and pressure recovery of 0.98 and 0.629. Determination of the flow conditions at the diffuser exit indicated that, in general, both diffusers had about the same degree of flow distortion. At or very near the critical pressure recovery of the diffusers the exit flow was reasonably good. However, as the operating point of either diffuser moved farther into the supercritical regime, considerable flow distortion was encountered.

INTRODUCTION

A full-scale free-jet investigation was conducted at the Lewis laboratory to evaluate and improve the performance of a 48-inch-diameter ramjet engine. The air is supplied to the ramjet engine through a side-inlet diffuser. The supersonic compression surface of the diffuser is essentially a 216° segment of a symmetric two-shock cone. The internal portion of the diffuser is contoured to turn the air and to diffuse it to the 32-inch-diameter diffuser-outlet station.

The first diffuser investigated was designed to produce a single oblique shock at the diffuser inlet. The performance of this diffuser

and the effectiveness of several devices to improve the diffuser-exit flow profiles are described in reference 1. A second diffuser designed by the manufacturer had two oblique shocks at the diffuser inlet. This report presents the performance of a heavy-duty full-scale version of the two-shock diffuser and compares these results with those obtained from the investigation of the single-shock inlet diffuser of reference 1.

Presentation of the performance of the two-shock diffuser is accomplished by giving its supercritical mass-flow ratio, critical diffuser pressure recovery, static-pressure profiles through the diffuser, and diffuser-outlet flow conditions. The investigation was conducted at a nominal free-stream Mach number of 2.75 over a range of inlet total pressures and temperatures of 3800 to 1930 pounds per square foot and 860° to 990° R, respectively. All the data were obtained during cold-flow supercritical diffuser operation at an angle of attack of zero.

APPARATUS

Installation

A sketch of the engine installed in the free-jet facility is presented in figure 1. Air to be supplied to the engine was brought to the desired pressure, temperature, and humidity through the use of compressors, heaters, and driers. This air was brought into a plenum chamber located ahead of the engine. The plenum chamber was separated from the test section by a bulkhead. A supersonic nozzle designed to produce a Mach number of 2.75 was placed so that its inlet was located in the plenum chamber and its exit was located in the test section. The pressure in the test chamber was reduced so as to establish a pressure ratio across the bulkhead high enough to accelerate the flow through the supersonic nozzle to the desired Mach number. The inlet of the diffuser was placed in the supersonic flow field. The air not captured by the inlet diffuser was diffused to test-section exhaust pressure by means of a jet diffuser. Details of this facility are given in reference 2.

Diffuser

Photographs of the two-shock diffuser are shown in figure 2. The supersonic portion was a 216° segment of a dual-cone (15° and 25° half-angles) Oswatitsch diffuser. Boundary-layer bleed air was ducted below the main diffuser to the facility exhaust section. Vortex generators used in the diffuser to improve the outlet flow profiles are described in figure 3. The flow area variation with diffuser length is shown in figure 4.

A description of the single-shock inlet diffuser is given in reference 1. The single-shock configuration used for comparison purposes herein is designated VG-2a in reference 1.

Exhaust Nozzle

The exhaust nozzle used during the investigation was a convergent-divergent nozzle and was equipped with a clamshell throttle downstream of the exhaust-nozzle exit. This clamshell throttle permitted diffuser pressure recovery to be varied during cold-flow operation. Airflow was measured at the throat of the choked exhaust nozzle. Screens were installed in the combustion chamber to ensure relatively uniform total-pressure profiles at the nozzle inlet.

Instrumentation

Details of the instrumentation are shown in figures 1 and 5. Diffuser-inlet conditions were measured at the inlet to the supersonic nozzle (station 0). The diffuser-outlet instrumentation station (station 3) was located at diffuser station 207, which is about 20 inches upstream of the combustor inlet. A shadowgraph installation was set up to observe the shock patterns at the entrance to the diffuser.

PROCEDURE

Data were obtained for the two-shock inlet diffuser at the following conditions: an inlet total temperature of 990° R at inlet total pressures of 1930, 2580, 3210, and 3800 pounds per square foot and an inlet total temperature of 860° R at an inlet total pressure of 2380 pounds per square foot. The diffuser pressure recovery was varied by means of the clamshell throttle mounted on the exhaust nozzle. Subcritical operation of the diffuser resulted in a flow breakdown from the supersonic free-jet nozzle. Consequently, all data were obtained between the most supercritical point of operation (i.e., clamshell nozzle wide open) and the diffuser critical point.

Symbols and methods of calculation are defined in appendixes A and B, respectively.

RESULTS AND DISCUSSION

Diffuser Mass-Flow Ratio

The supercritical mass-flow ratio of the two-shock inlet diffuser was calculated to be 0.992 (see appendix B). This was substantially in

agreement with the observed position of the shock system at the diffuser inlet. The mass-flow ratio of the single-shock inlet diffuser was about 0.98 (ref. 1).

Critical Pressure Recovery

Critical recovery of the two-shock inlet diffuser was found to be 0.643. This was slightly over 2 percent better than the critical recovery of 0.629 observed with the single-shock inlet diffuser (ref. 1). This increase in critical diffuser pressure recovery would be expected to increase the missile range about 1 percent.

Diffuser Static-Pressure Variation

The data presented in figure 6 show the variation of static pressures through the two-shock diffuser at several different diffuser pressure recoveries at an inlet total pressure of 2580 pounds per square foot and an inlet total temperature of 990° R. The data of figure 6(a) are internal static pressures on the diffuser outer surface, while the data of figure 6(b) are static pressures on the diffuser innerbody. Inasmuch as there is a static-pressure rise across a normal shock, the position of the shock system in the diffuser can be ascertained from the data shown in figure 6.

Diffuser-Outlet Flow Conditions

Conditions at the exit of the diffuser are very important because they directly affect the performance of the combustor. Distortion of the flow at the diffuser exit may result in high combustor pressure losses, reduced combustor efficiency, and in severe cases, burning upstream of the flameholding elements. Two approaches are used to present the flow conditions at the diffuser exit. The first of these is simply the presentation of diffuser-pressure-recovery and Mach number contours at the diffuser exit. These contours are presented in figure 7 for the two-shock inlet diffuser at several different average diffuser pressure recoveries for a free-stream total pressure of 2580 pounds per square foot and a free-stream total temperature of 990° R. The Mach number contours are expressed as the ratio $\frac{M_l - M_{av}}{M_{av}}$. The contours show that as the average diffuser pressure recovery is reduced from its critical value, the flow distortions at the diffuser outlet become quite severe, even to the point of a small area of flow separation or reversal (e.g., at an average pressure recovery of 0.500).

The second method of evaluating the flow conditions at the diffuser exit is presented in figure 8 where at several diffuser-inlet conditions the ratio of static to total pressure at the diffuser exit is shown as a function of diffuser total-pressure recovery for the two-shock diffuser. In addition to the data points shown on this figure, there is a dashed curve (plotted by the method in appendix B) that indicates the ideal (uniform flow) relation between the two parameters. Thus, as the diffuser-exit flow becomes more and more distorted, the diffuser operating point will move farther and farther away from the ideal curve. A further explanation of the meaning of these parameters is given in reference 1. The data of figure 8 show that at a diffuser-inlet pressure of 3800 pounds per square foot there was less flow distortion at the diffuser exit than at diffuser-inlet pressures from 1930 to 3210 pounds per square foot. The results described by the data of figure 8 substantiate the contours shown in figure 7. The chief advantage of the method of presentation in the latter figure is that a criterion is available for expressing the flow uniformity as a single number, and thus trends and comparisons are more readily shown.

A comparison between the diffuser-exit flow conditions for the two-shock and single-shock inlet diffuser is given in figures 9 and 10 by the two methods of presentation just discussed. The contours of figure 9 compare the two diffusers at their respective critical recoveries. These contours indicate that the diffuser-exit flow conditions at critical recovery were about the same for both the single-shock and the two-shock diffusers.

Further comparison is presented in figure 10 by a plot in generalized form of the diffuser-outlet static- to total-pressure ratio as a function of diffuser recovery. Instead of using the same coordinates as used to present the two-shock inlet-diffuser data, an attempt has been made to generalize the data in order to make the comparison more direct. Consequently, for each diffuser the measured diffuser-outlet static- to total-pressure ratio has been divided by the ideal ratio and the diffuser recovery is given in terms of its relation to the critical recovery. In figure 10, which presents data for free-stream total pressure and temperature of 2580 pounds per square foot and 990° R, respectively, the dashed line represents a curve drawn through the data given in reference 1. The solid line represents the curve drawn through the appropriate data points presented in figure 8. In general, the data indicate both diffusers had about the same degree of diffuser-exit flow distortion when they were operated at the same point with respect to their critical operating point. This is in agreement with the contours presented in figure 9.

SUMMARY OF RESULTS

An investigation was made to determine the performance of a two-shock inlet diffuser which was to be used in conjunction with a 48-inch-diameter ramjet engine. The supercritical mass-flow ratio of this inlet diffuser was about 0.99, and its critical pressure recovery was 0.643. Corresponding values of 0.98 and 0.629 were observed for a single-shock inlet diffuser designed for the same engine. Determination of the flow conditions at the exit of the diffuser indicated that, in general, both diffusers had about the same degree of flow distortion. At or very near the critical pressure recovery of the diffusers the exit flow was reasonably good. However, as the operating point of either diffuser moved farther into the supercritical regime considerable flow distortion was encountered.

Lewis Flight Propulsion Laboratory
National Advisory Committee for Aeronautics
Cleveland, Ohio, February 1, 1957

APPENDIX A

SYMBOLS

The following symbols are used in this report:

A	cross-section area, sq ft
g	acceleration due to gravity, 32.2 ft/sec^2
M	Mach number
P	total pressure, lb/sq ft abs
p	static pressure, lb/sq ft abs
R	gas constant, 53.4 ft-lb/(lb)(^oR)
T	total temperature, ^oR
t	static temperature, ^oR
V	velocity, ft/sec
w	airflow, lb/sec
γ	ratio of specific heats
ρ	density, lb/cu ft

Subscripts:

av	average
l	local
0	free stream (inlet to supersonic nozzle)
1	supersonic diffuser inlet
3	diffuser outlet station

APPENDIX B

METHODS OF CALCULATION

Diffuser Supercritical Mass-Flow Ratio

Mass flow in the stream tube approaching the diffuser inlet is given by

$$w_0 = \rho_0 A_1 V_0 = \frac{p_0}{Rt_0} A_1 M_0 \sqrt{\gamma_0 g R t_0} = \sqrt{\frac{\gamma_0 g}{R}} \frac{p_0}{\sqrt{T_0}} A_1 \left[\frac{M_0}{\left(1 + \frac{\gamma - 1}{2} M_0^2\right)^{\frac{\gamma_0 + 1}{2(\gamma_0 - 1)}}} \right]$$

For $M_0 = 2.75$, $\gamma_0 = 1.4$, and A_1 (capture area) = 6.19 square feet,

$$w_0 = 0.987 \frac{p_0}{\sqrt{T_0}}$$

Airflow calibration of the engine showed that the engine airflow is given by

$$w_0 = 0.980 \frac{p_0}{\sqrt{T_0}}$$

Thus the supercritical mass-flow ratio is 0.992.

Diffuser Total-Pressure Recovery

Diffuser total-pressure recovery was taken as the ratio of the average total pressure measured at the diffuser-outlet instrumentation station (station 3) to the average total pressure measured at the inlet of the supersonic nozzle (station 0). Since the pressure tubes at station 3 were placed at centers of equal areas, area average rather than mass-flow average values of pressure were obtained. Any total-pressure losses occurring in the supersonic nozzle were attributed to the diffuser. When the flow at station 3 was partly supersonic, no corrections were made for shock losses at the total-pressure tubes.

Diffuser-Outlet Mach Number Profiles

Mach numbers were calculated for each total-pressure tube at station 3 from the ratio of static to total pressure with 1.38 as the ratio of specific heats. A small circumferential gradient was found in the wall static pressures at this station. Accordingly, the average of these pressures was assumed to exist on the duct centerline, and the static pressure at each total-pressure probe location was found by linear interpolation from the centerline to the individual wall static tap associated with the particular total-pressure rake under consideration.

Ideal Variation of Diffuser-Outlet Static- to Total-Pressure Ratio with Diffuser Total-Pressure Recovery

The ideal variation of p_3/P_3 with P_3/P_0 can be obtained by relating both ratios to the diffuser-outlet Mach number. Diffuser recovery P_3/P_0 can be related to Mach number as follows:

$$w_3 = \rho_3 A_3 V_3 = \frac{\sqrt{\frac{\gamma_3 g}{R}}\, P_3 A_3}{\sqrt{T_3}} \left[\frac{M_3}{\left(1 + \frac{\gamma_3 - 1}{2} M_3^2\right)^{\frac{\gamma_3+1}{2(\gamma_3-1)}}} \right] \tag{1}$$

Also, from an airflow calibration of the diffuser,

$$w_3 = w = 0.980 \frac{P_0}{\sqrt{T_0}} \tag{2}$$

Assuming that $T_3 = T_0$ and setting the right sides of equations (1) and (2) equal give

$$\frac{0.980\, P_0}{\sqrt{T_3}} = \frac{\sqrt{\frac{\gamma_3 g}{R}}\, P_3 A_3}{\sqrt{T_3}} \left[\frac{M_3}{\left(1 + \frac{\gamma_3 - 1}{2} M_3^2\right)^{\frac{\gamma_3+1}{2(\gamma_3-1)}}} \right] \tag{3}$$

Algebraic manipulation gives

$$P_3/P_0 = \frac{0.980}{\sqrt{\frac{\gamma_3 g}{R}}\, A_3}\left[\frac{\left(1 + \frac{\gamma_3 - 1}{2} M_3^2\right)^{\frac{\gamma_3+1}{2(\gamma_3-1)}}}{M_3}\right] \tag{4}$$

and

$$\frac{p_3}{P_3} = \left(1 + \frac{\gamma_3 - 1}{2} M_3^2\right)^{-\frac{\gamma_3}{\gamma_3-1}} \tag{5}$$

Using equations (4) and (5), $\gamma = 1.38$, and $A_3 = 4.32$ square feet and assuming various values of M_3 permit calculation of corresponding values of p_3/P_3 and P_3/P_0.

REFERENCES

1. Farley, John M., and Seashore, Ferris L.: Full-Scale, Free-Jet Investigation of Methods of Improving Outlet Flow Distribution in a Side-Inlet Supersonic Diffuser. NACA RM E54L31a, 1955.

2. Seashore, Ferris L., and Hurrell, Herbert G.: Starting and Performance Characteristics of a Large Asymmetric Supersonic Free-Jet Facility. NACA RM E54A19, 1954.

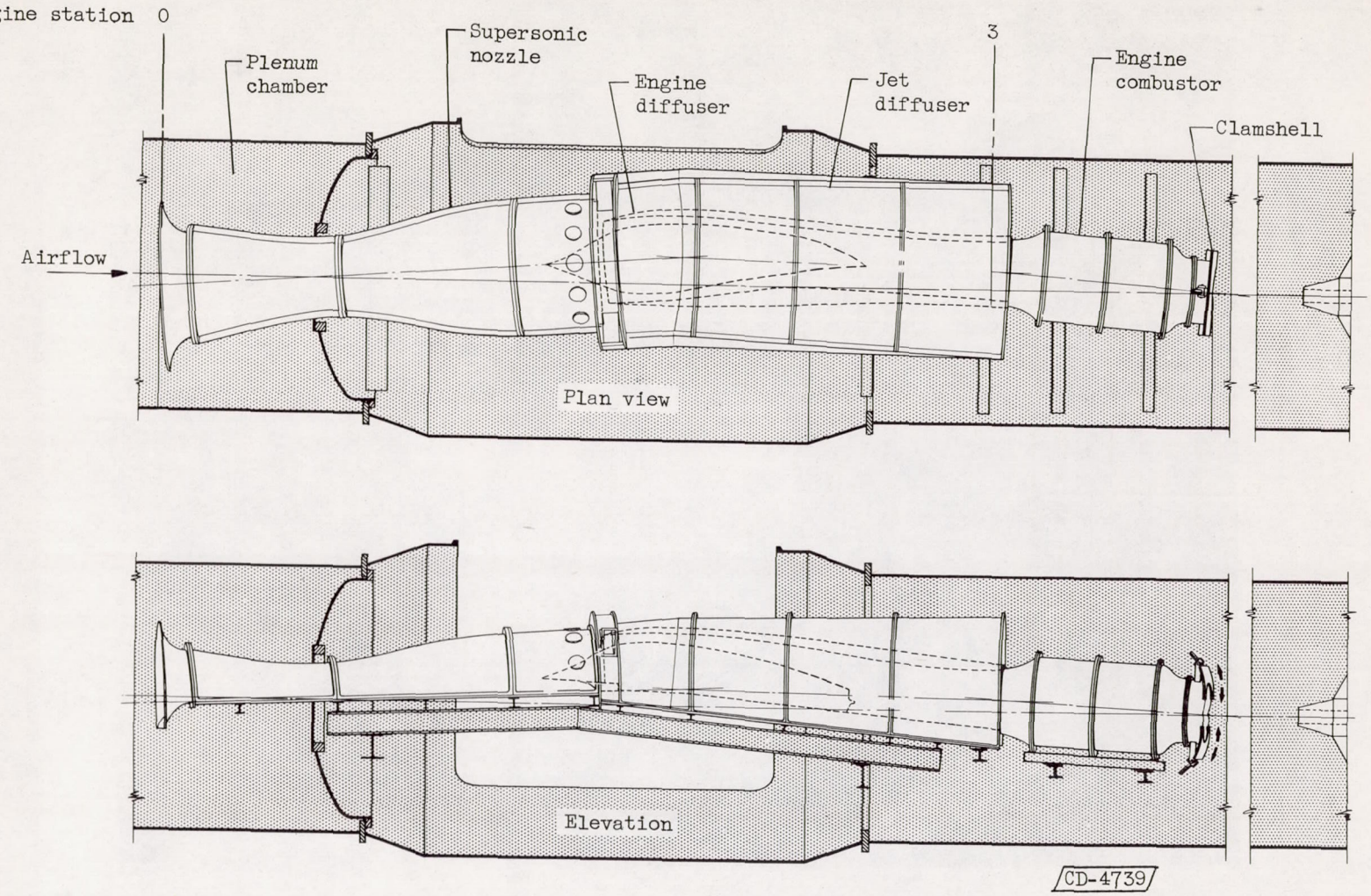

Figure 1. - Free-jet test facility and engine installation.

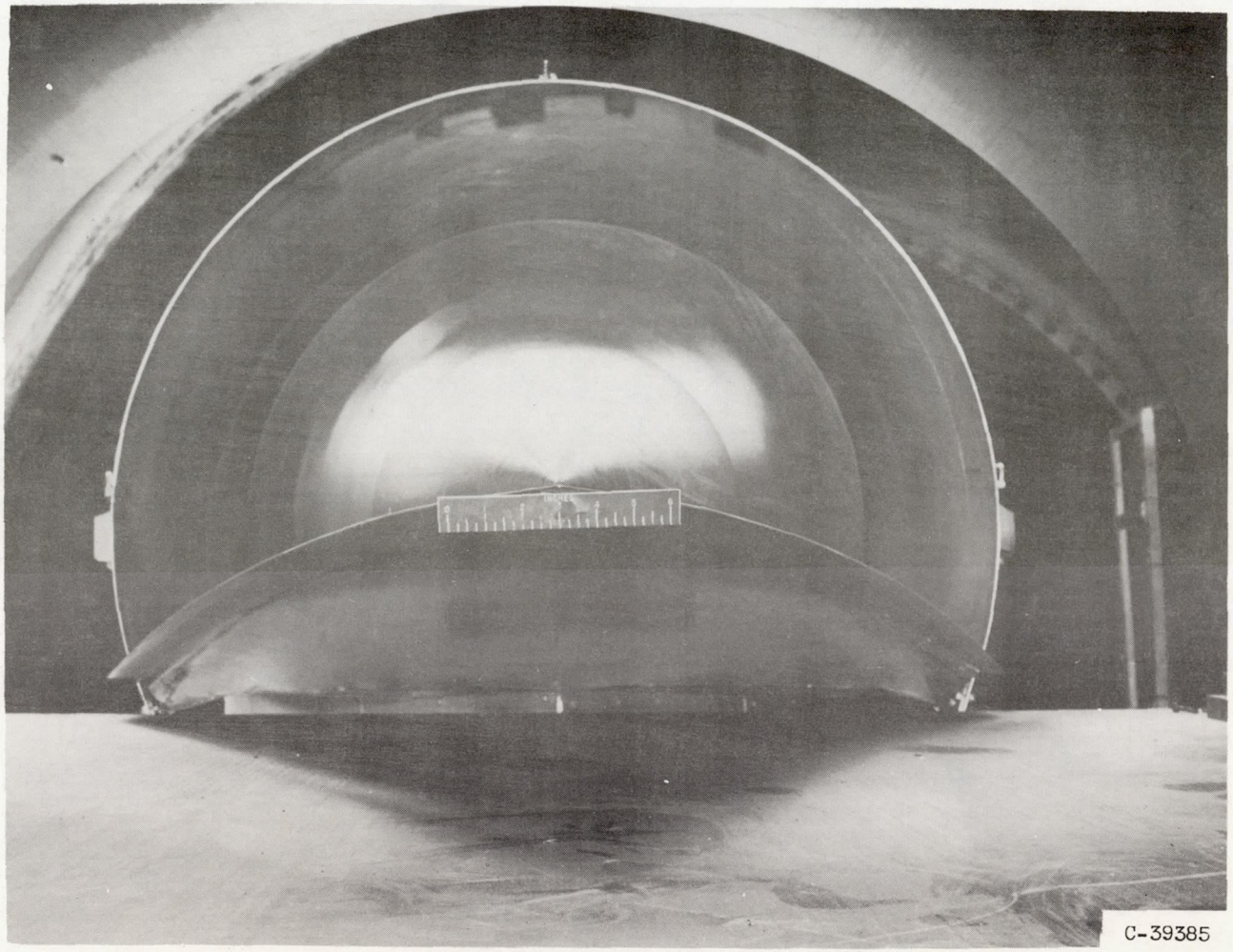

(a) Diffuser inlet (looking downstream).

Figure 2. - Two-shock inlet diffuser.

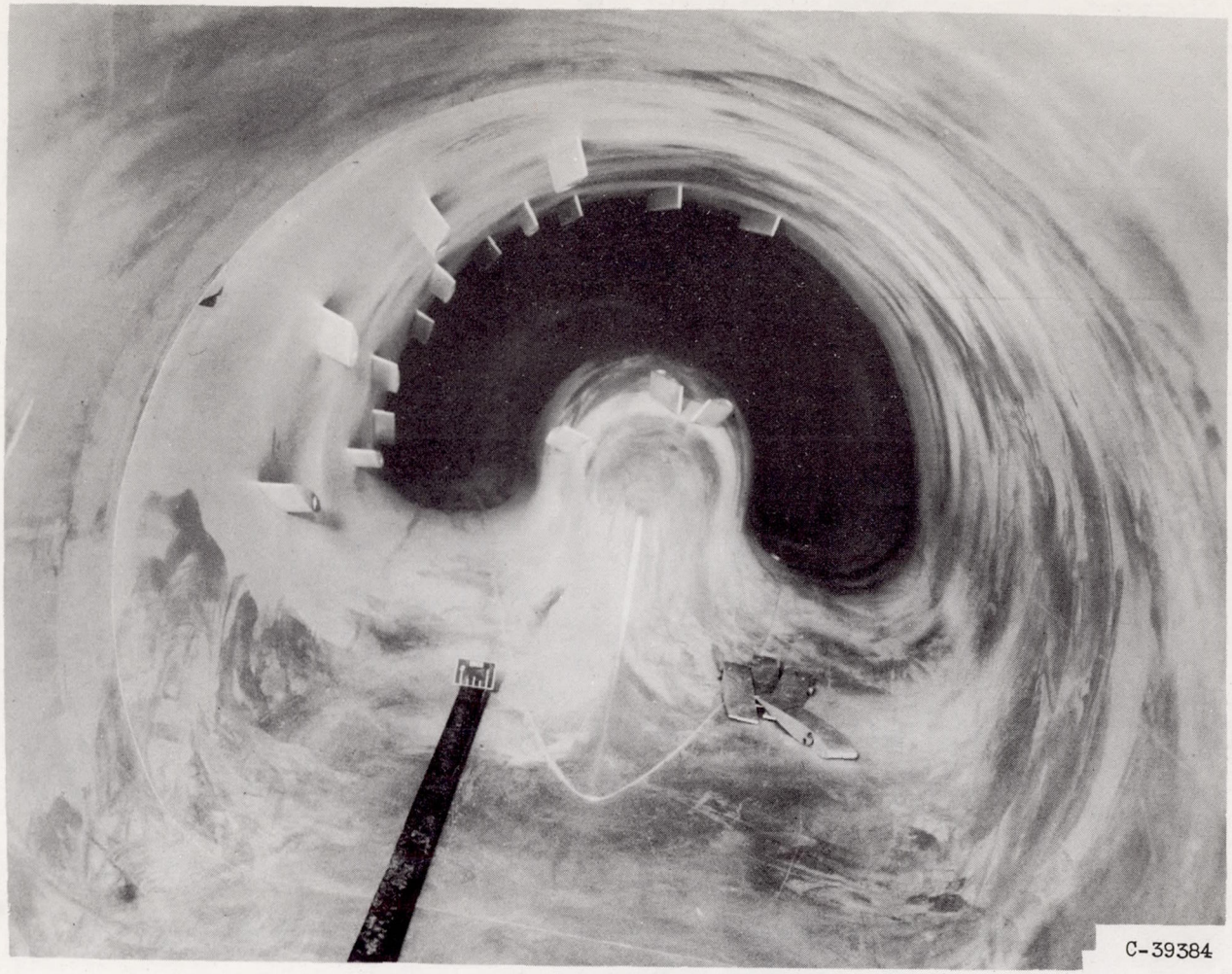

(b) Diffuser outlet (looking upstream).

Figure 2. - Concluded. Two-shock inlet diffuser.

Section	Vortex generator Span, in.	Cord, in.
C-C	0.800	4.00
D-D	1.074	6.00
H-H	1.180	6.00
J-J	1.180	6.00
K-K	1.350	6.00
M-M	1.350	6.00

Generator trailing edge faces right at odd numbered locations and left at even numbered locations, as indicated by arrows

Numbers on each section indicate equal divisions on cowl or innerbody surface

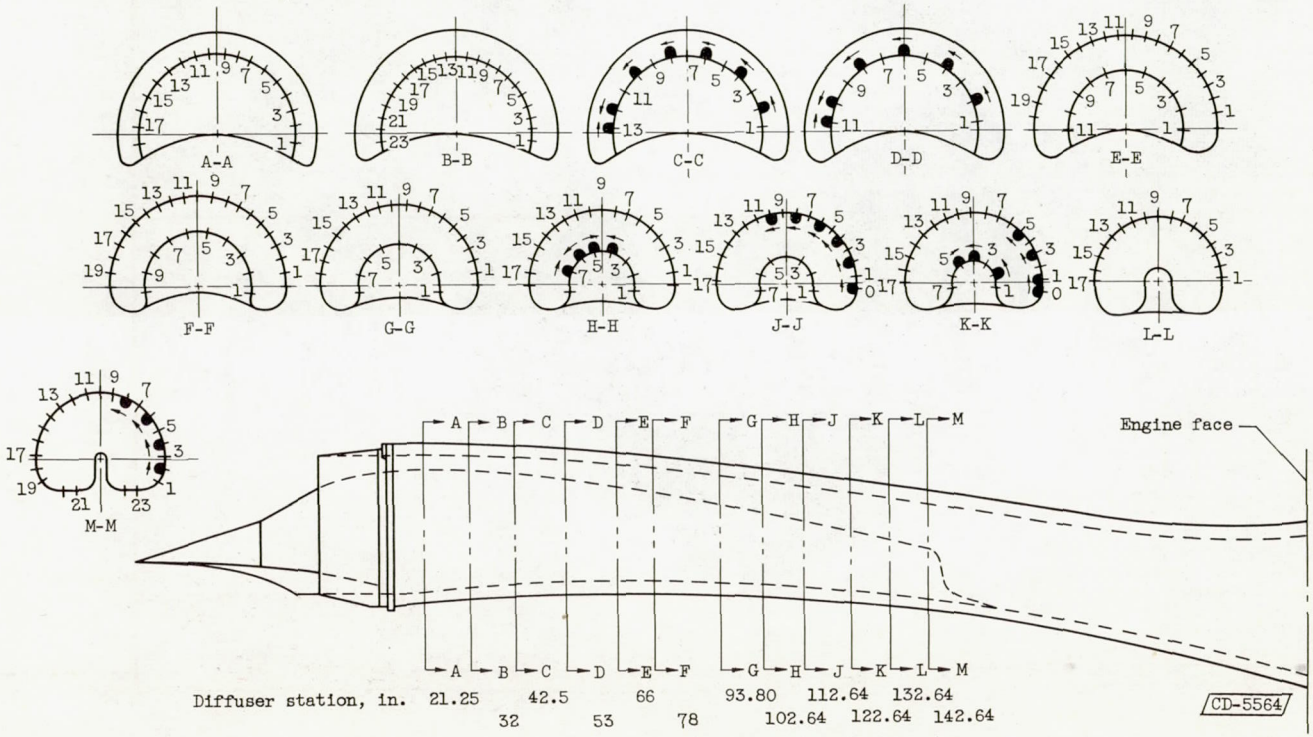

Figure 3. - Vortex-generator locations.

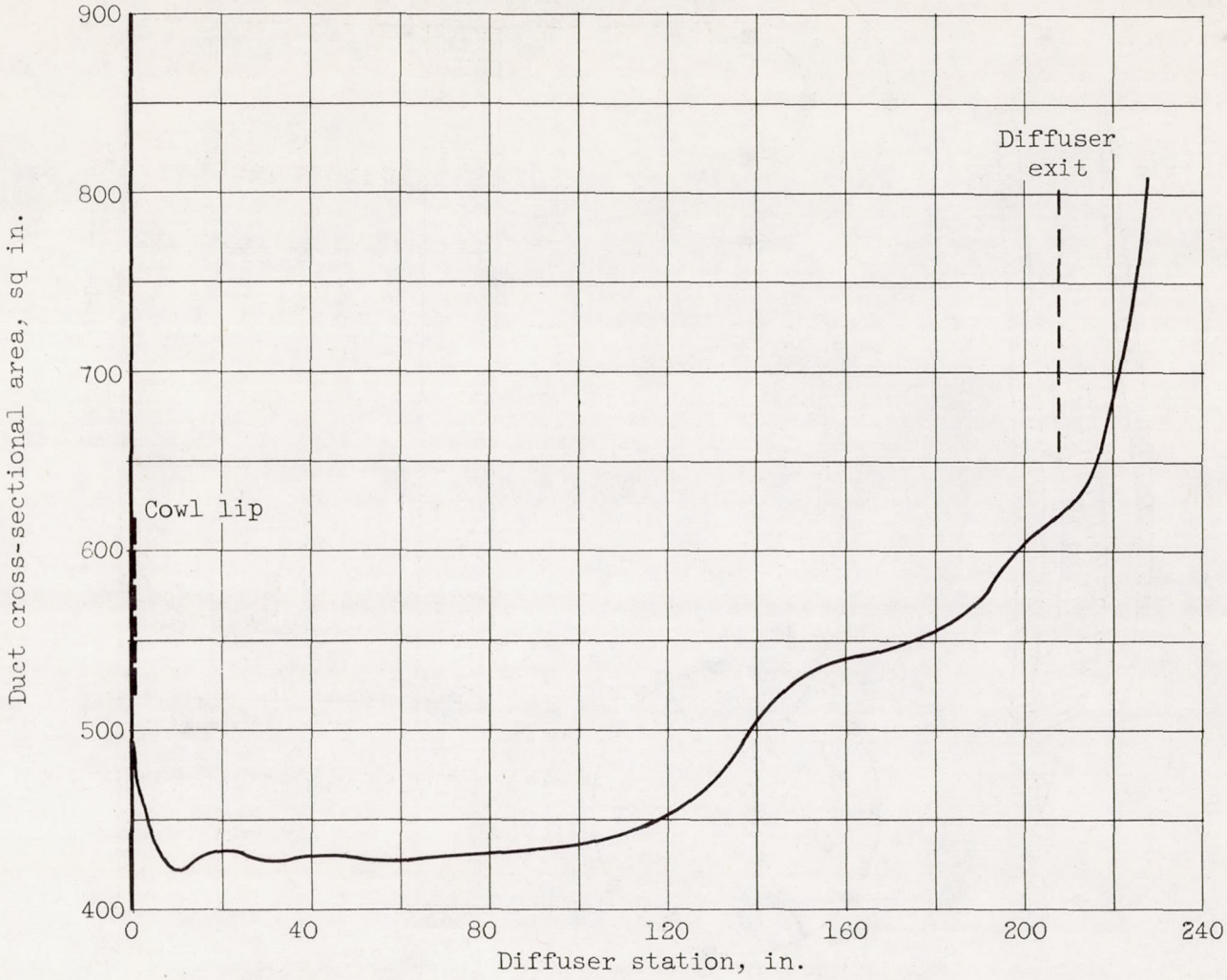

Figure 4. - Variation of diffuser cross-sectional area.

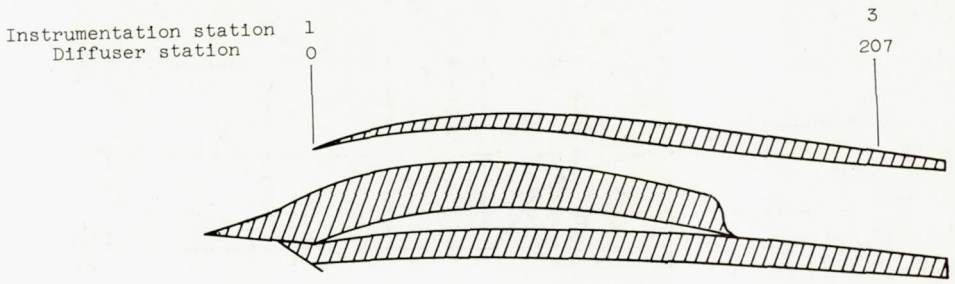

(a) Side view of diffuser.

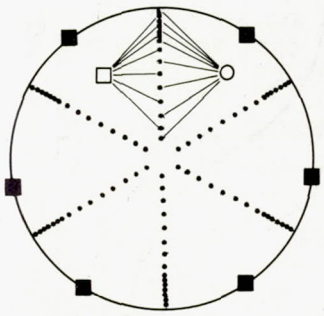

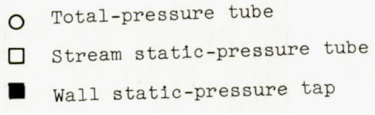

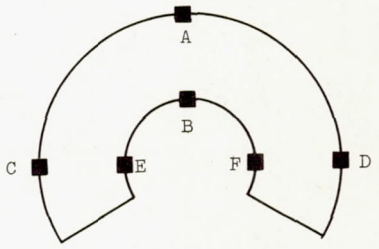

(b) Diffuser-outlet instrumentation station (station 3) (looking downstream).

(c) Typical section (looking downstream).

Diffuser station	Circumferential location of static-pressure taps	Diffuser station	Circumferential location of static-pressure taps
-36	B	24	ABCDEF
-25	B	30	AB
-16	B	34	AB
-12	B	39	AB
-4	B	45	ABCDEF
0	ABCDEF	60	AB
5	AB	75	ABCD
7	ABCDEF	90	AB
9	AB	105	ABCD
11	BEF	121	ABCD
12	ACD	138	ABCD
14	AB	154	ABCD
17	ABCDEF	165	AB
19	AB	183	ABCD
22	AB	207	ABCDEF

Figure 5. - Location of diffuser instrumentation.

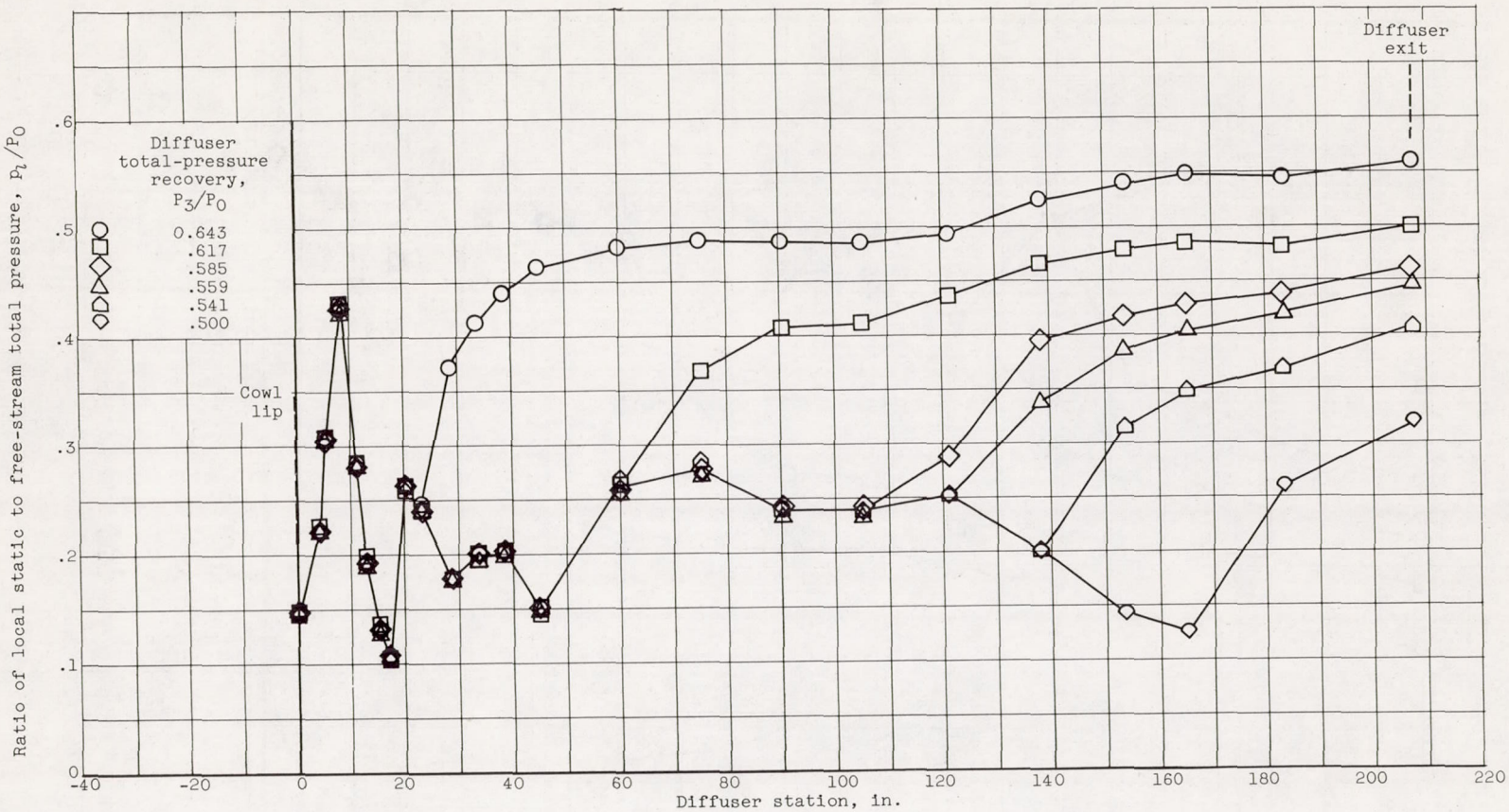

(a) Diffuser outer surface.

Figure 6. - Variation of ratio of local static to free-stream total pressure through diffuser at several diffuser pressure recoveries. Free-stream total pressure, 2580 pounds per square foot; free-stream total temperature, 990° R.

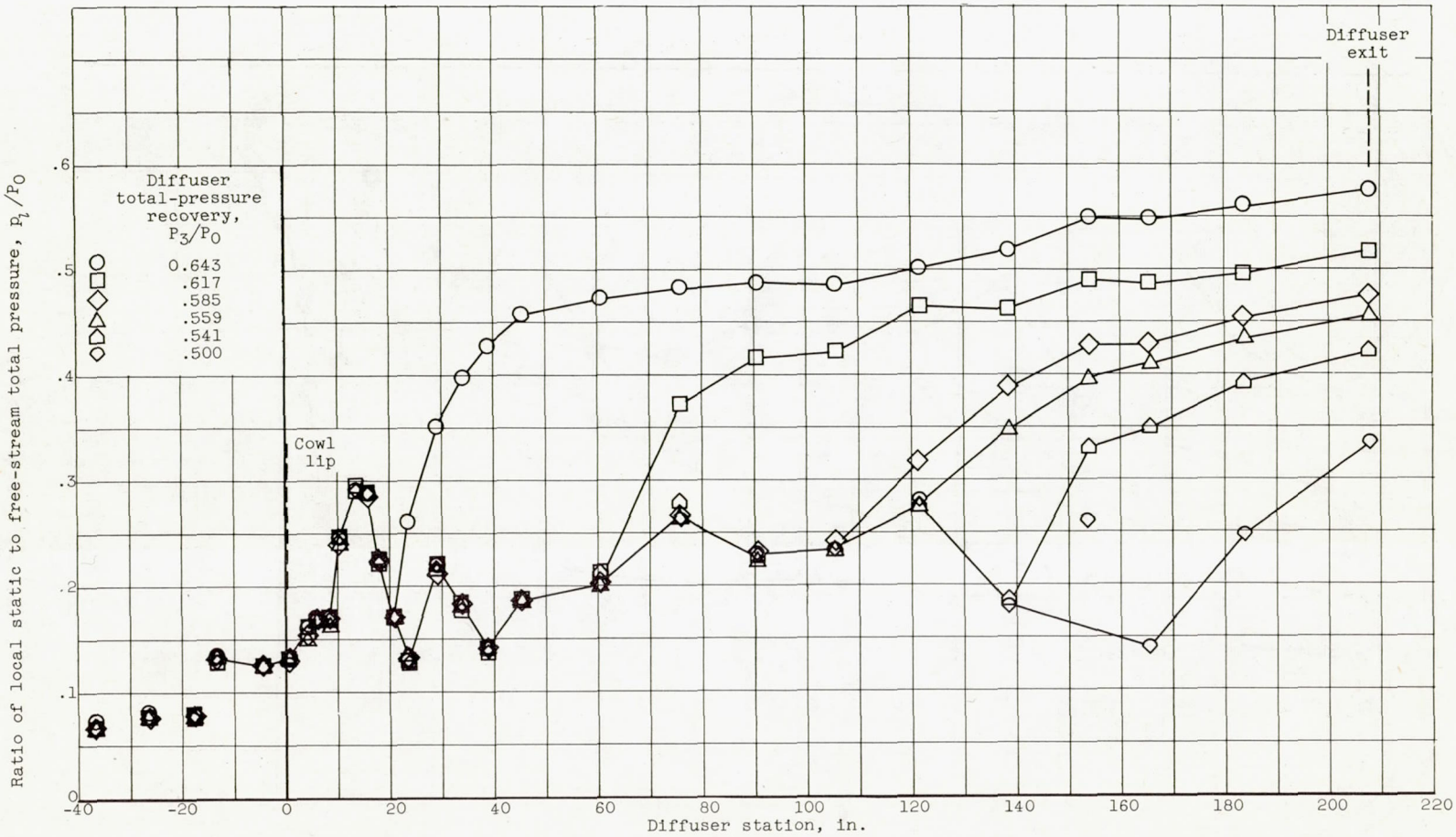

(b) Diffuser innerbody.

Figure 6. - Concluded. Variation of ratio of local static to free-stream total pressure through diffuser at several diffuser pressure recoveries. Free-stream total pressure, 2580 pounds per square foot; free-stream total temperature, 990° R.

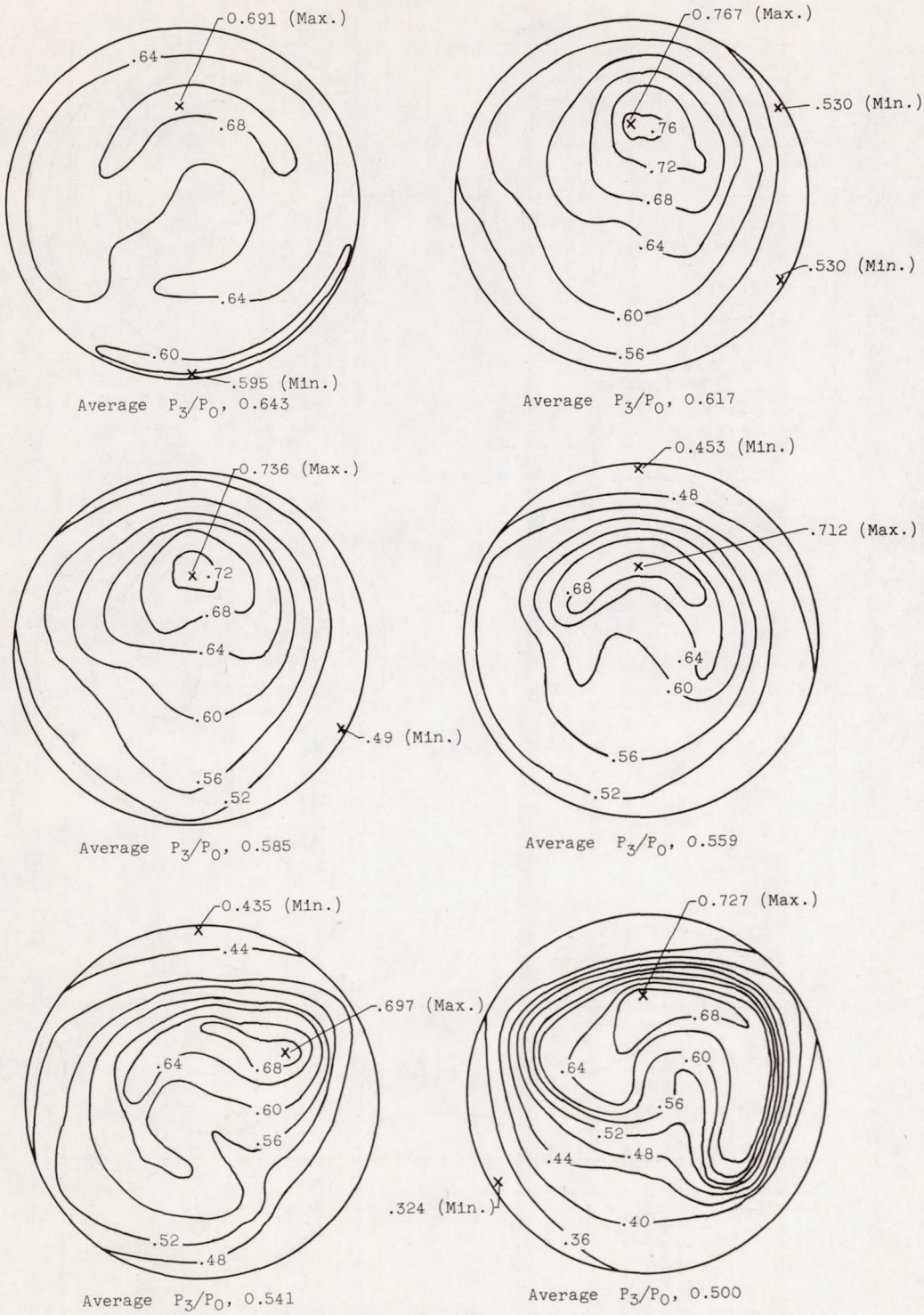

(a) Contours of diffuser pressure recovery, P_3/P_0.

Figure 7. - Diffuser-outlet contours for two-shock diffuser. Free-stream total pressure, 2580 pounds per square foot; free-stream total temperature, 990° R; view looking downstream.

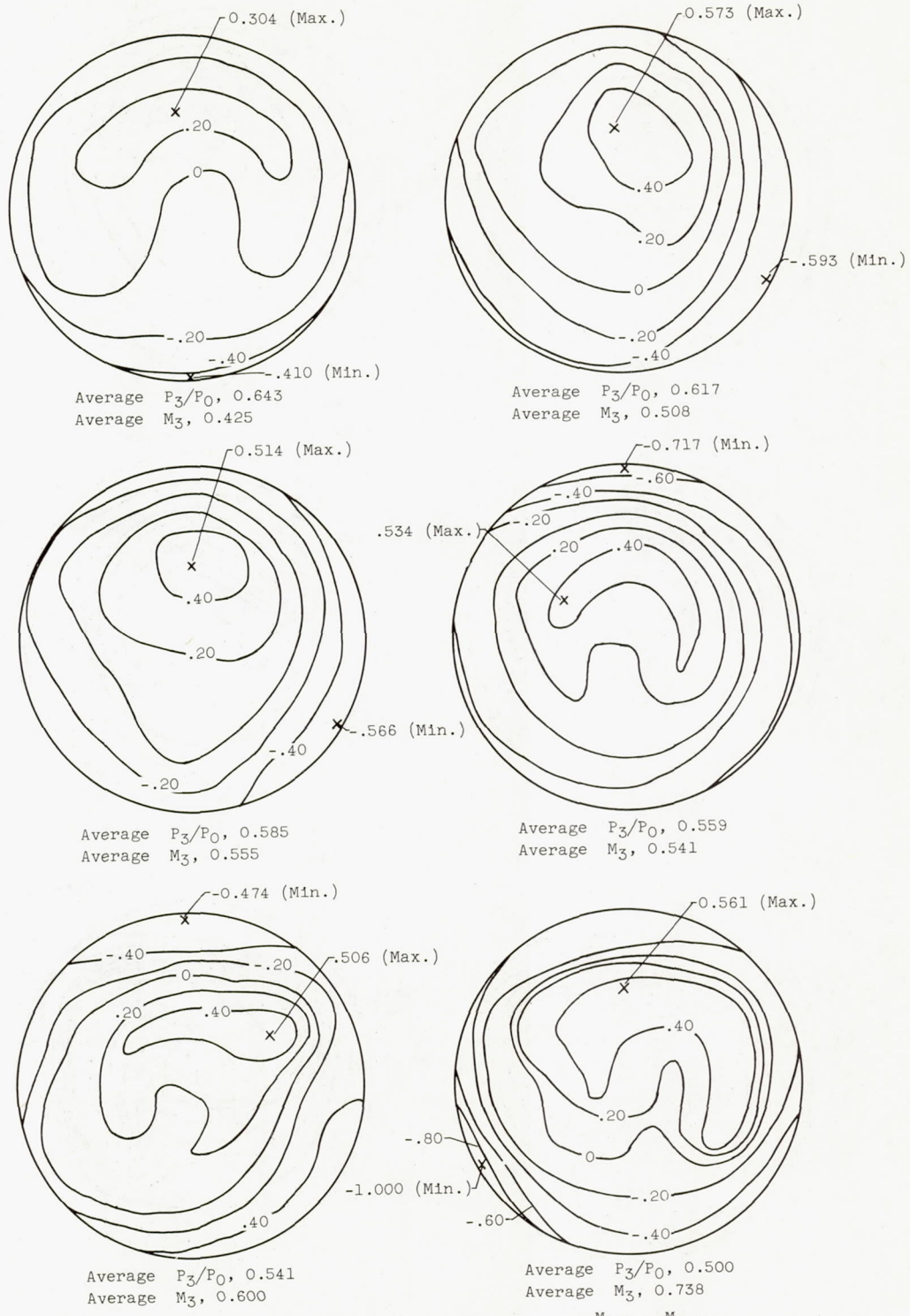

(b) Contours of diffuser Mach number parameter, $\frac{M_{3,l} - M_{3,av}}{M_{3,av}}$.

Figure 7. - Concluded. Diffuser-outlet contours for two-shock diffuser. Free-stream total pressure, 2580 pounds per square foot; free-stream total temperature, 990° R; view looking downstream.

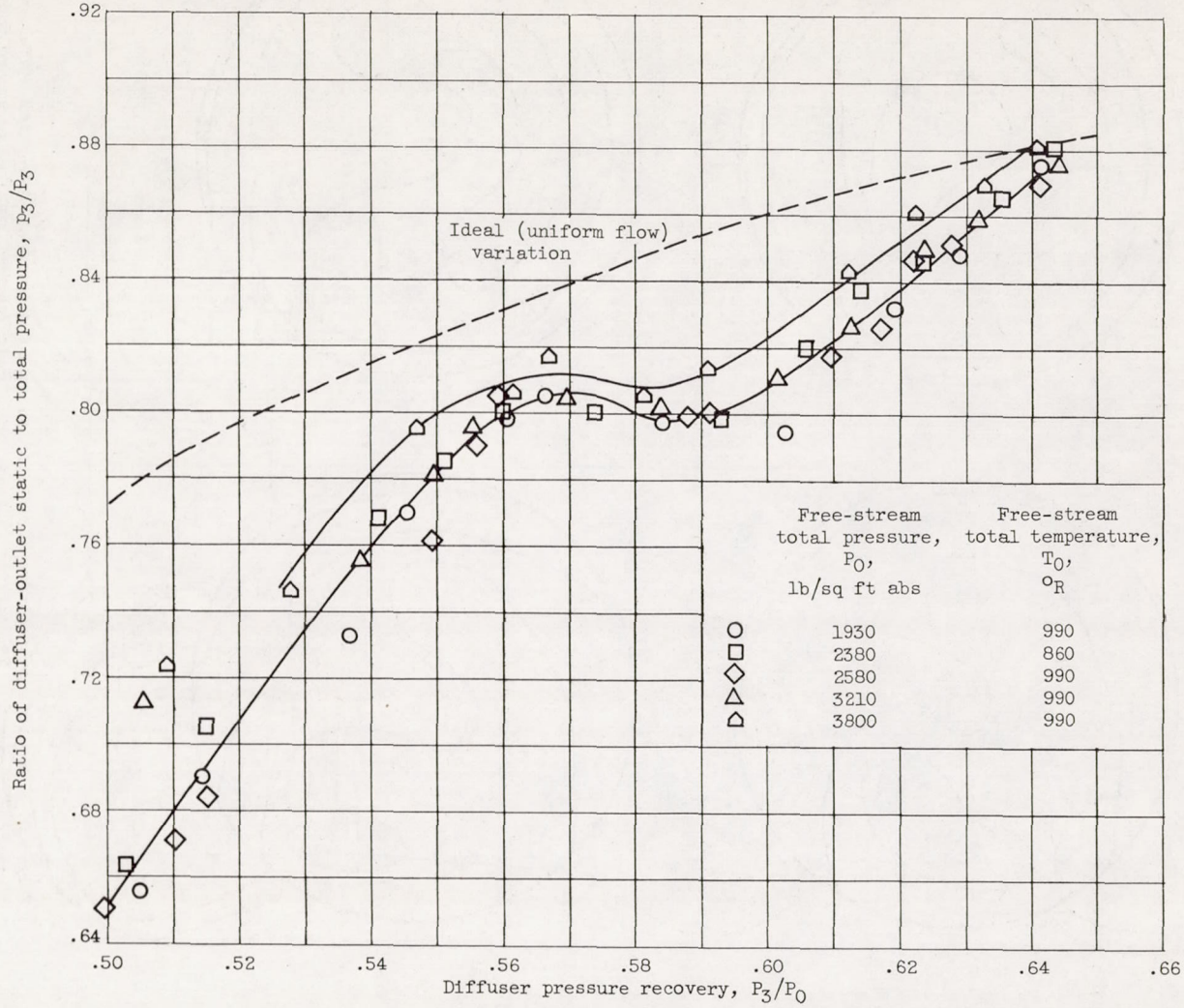

Figure 8. - Variation of ratio of diffuser-outlet static to total pressure with diffuser pressure recovery for two-shock inlet diffuser.

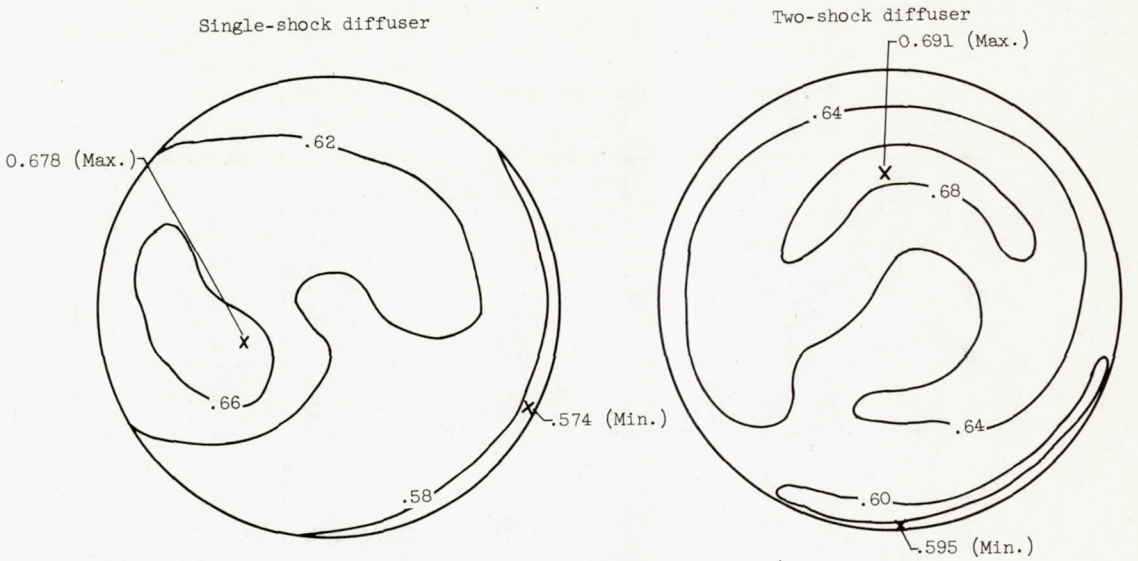

(a) Diffuser pressure recovery, P_3/P_0.

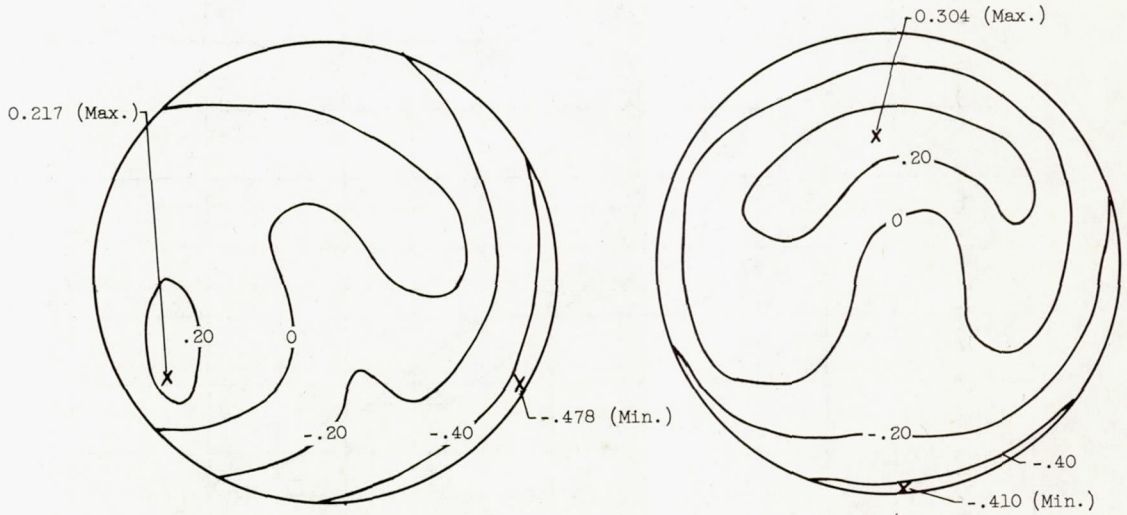

Average P_3/P_0, 0.629
Average M_3, 0.460

Average P_3/P_0, 0.643
Average M_3, 0.425

(b) Diffuser Mach number parameter, $\frac{M_{3,l} - M_{3,av}}{M_{3,av}}$.

Figure 9. - Comparison of diffuser-outlet contours of single- and two-shock diffusers at critical recovery. Nominal free-stream total pressure, 2580 pounds per square foot absolute; nominal free-stream total temperature, 990° R.

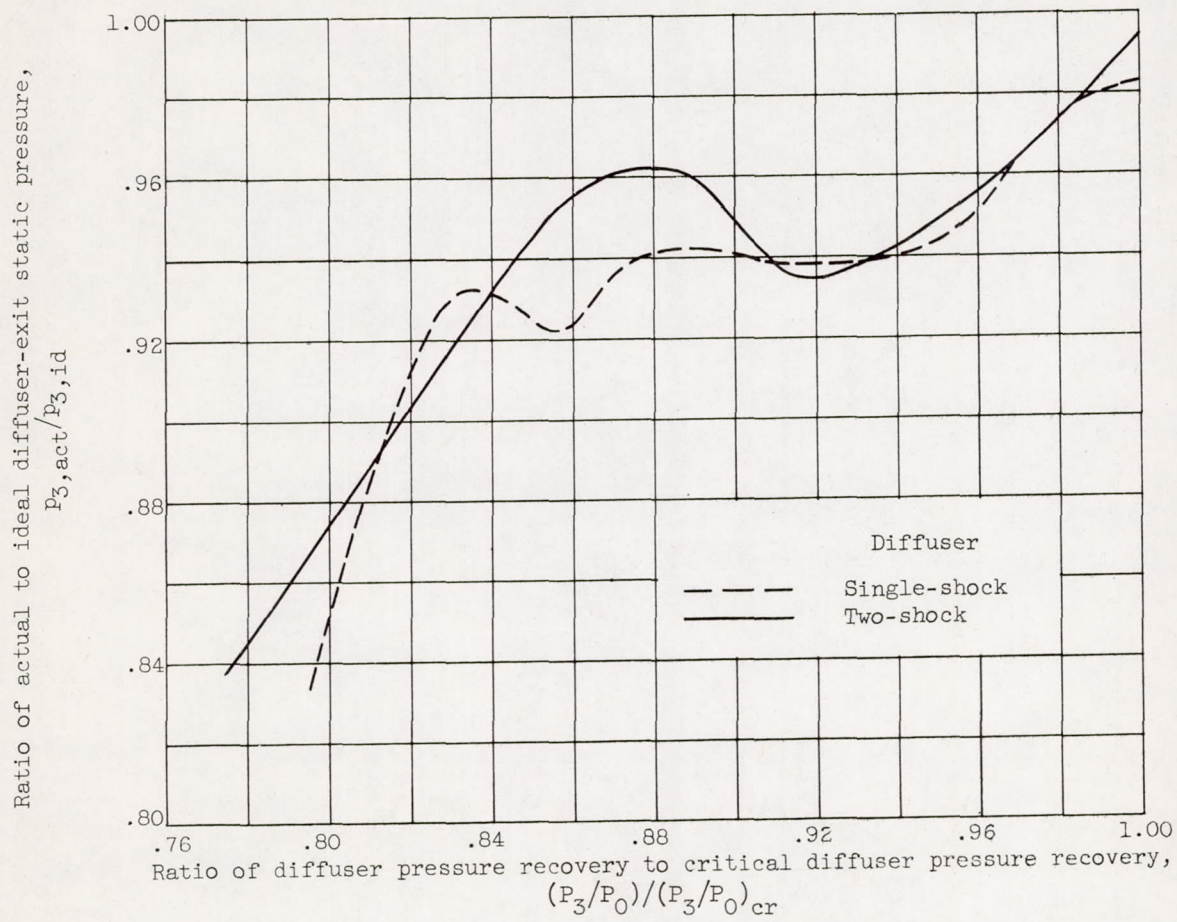

Figure 10. - Comparison of flow distortion at diffuser exit for single- and two-shock diffusers. Nominal free-stream total pressure, 2580 pounds per square foot absolute; nominal free-stream total temperature, 990° R.